

The EUMETSAT
Network of
Satellite
Application
Facilities



CM SAF

Climate Monitoring

Validation Report

Fundamental Climate Data Record of SSMI / SSMIS Brightness Temperatures

DOI: [10.5676/EUM_SAF_CM/FCDR_MWI/V002](https://doi.org/10.5676/EUM_SAF_CM/FCDR_MWI/V002)

Microwave Radiance FCDR R2

CM-12001

Reference Number:


SAF/CM/DWD/VAL/FCDR_SSMIS

Issue/Revision Index:

1.1

Date:

2015-02-26

	EUMETSAT SAF on CLIMATE MONITORING Validation Report Microwave Radiance FCDR R2	Doc.No.: SAF/CM/DWD/VAL/FCDR_SSMIS Issue: 1.1 Date: 2015-02-26
---	--	--

Document Signature Table

	Name	Function	Signature	Date
Author	Karsten Fennig	CM SAF scientist		2015-02-26
Editor	Marc Schröder	DRR Coordinator		2015-02-26
Approval	Rainer Hollmann	Science Coordinator		2015-02-27
Release	Martin Werscheck	Project Manager		



Distribution List

Internal Distribution	
Name	No. Copies
DWD Archive	1
CM SAF Team	1

External Distribution		
Company	Name	No. Copies
PUBLIC		1

Document Change Record

Issue/Revision	Date	DCN No.	Changed Pages/Paragraphs
1.0	2014-11-27	SAF/CM/DWD/VAL/FCDR_SSMIS	Version for review.
1.1	2015-02-26	SAF/CM/DWD/VAL/FCDR_SSMIS	Final version after DRR.

 	EUMETSAT SAF on CLIMATE MONITORING Validation Report Microwave Radiance FCDR R2	Doc.No.: SAF/CM/DWD/VAL/FCDR_SSMIS Issue: 1.1 Date: 2015-02-26
---	--	--

Applicable documents

Reference	Title	Code / Validity Date
AD 1	Memorandum of Understanding between CM SAF and the Max-Planck Institute for Meteorology and Meteorological Institute, University of Hamburg	1. March 2012
AD 2	CM SAF Product Requirements Document	SAF/CM/DWD/PRD/2.4

Reference documents

Reference	Title	Code
RD 1	Product User Manual Fundamental Climate Data Record of SSMI / SSMIS Brightness Temperatures	SAF/CM/DWD/PUM/FCDR_SSMIS/1.1
RD 2	Algorithm Theoretical Basis Document Fundamental Climate Data Record of SSMI / SSMIS Brightness Temperatures	SAF/CM/DWD/ATBD/FCDR_SSMIS/1.1
RD 3	Algorithm Theoretical Basis Document Fundamental Climate Data Record of SSMI / Brightness Temperatures	SAF/CM/DWD/ATBD/FCDR_SSMI/1.3
RD 4	Product User Manual Fundamental Climate Data Record of SSMI / Brightness Temperatures	SAF/CM/DWD/ATBD/FCDR_SSMI/1.0
RD 5	Validation Report Fundamental Climate Data Record of SSMI / Brightness Temperatures	SAF/CM/DWD/VAL/FCDR_SSMI/1.0





 	EUMETSAT SAF on CLIMATE MONITORING Validation Report Microwave Radiance FCDR R2	Doc.No.: SAF/CM/DWD/VAL/FCDR_SSMIS Issue: 1.1 Date: 2015-02-26
---	--	--

Table of Contents

List of Figures	5
List of Tables.....	5
I Preface	7
I-1 The EUMETSAT SAF on Climate Monitoring.....	7
I-2 Introduction	7
II SSM/I.....	8
III SSMIS	9
III-1 Instrument and sensor stability.....	9
III-2 Evaluation of Brightness Temperature differences.....	10
III-2.1 Data Sets for Comparison	11
III-2.2 Visual inspection	13
III-2.3 Evaluation strategy	15
III-2.4 Evaluation Results	18
III-3 Conclusions.....	33
III-4 References.....	34
III-5 Glossary	35

 	EUMETSAT SAF on CLIMATE MONITORING Validation Report Microwave Radiance FCDR R2	Doc.No.: SAF/CM/DWD/VAL/FCDR_SSMIS Issue: 1.1 Date: 2015-02-26
---	--	--

List of Figures

Figure 1: Time series of DMSP platform mean local equator crossing times, altitude and the Earth Incidence Angles of the different SSMIS instruments. Thin lines are the mean values at the ascending equator crossing and thick lines depict complete orbit mean values. Colours are as follows: F16 orange, F17 blue, F18 black.	10
Figure 2: Time series of SSMIS sensor diagnostics: Temperature of the warm calibration target (upper panel) and temperature of the reflector arm (lower panel). The grey lines denote 0°C (for colours see Figure 1).....	11
Figure 3: Time series of SSMIS sensor diagnostics: Radiometer sensitivities for the channels at 19v, 19h, 22v, 37v, 37h, 91v and 91h GHz. The grey lines denote the specification values for colours see Figure 1).	12
Figure 4: Climatological mean of TB differences at 19 GHz between SSM/I F13 and SSMIS F16. The left column shows the original uncorrected raw data records. The middle column depicts the CM SAF FCDR and the right column shows the CSU FCDR. The top row shows the vertical polarisation, the middle row the horizontal polarisation and the bottom row depicts the double differences between both polarisations.	14
Figure 5: As Figure 4 but for the SSMIS TB differences at 19 GHz between F17 and F18.....	15
Figure 6: Time series of ensemble anomalies and variability for SSM/I & SSMIS channel 19v GHz. In the upper two panels the solid lines are PM orbits and the dashed lines AM orbits. The lower panels depict daily means of AM and PM orbits. The gray lines depict the ensemble spread. Horizontal dotted grey lines denote the optimal and target bias. For a detailed description see text (section III-2.3). Colours are as in Figure1 plus green (F13) and purple (F14).....	19
Figure 7: Same as Figure 6, but for SSM/I & SSMIS channel 19h GHz.	21
Figure 8: Same as Figure 6, but for SSM/I & SSMIS channel 22v GHz.	23
Figure 9: Same as Figure 6, but for SSM/I & SSMIS channel 37v GHz.	25
Figure 10: Same as Figure 6, but for SSM/I & SSMIS channel 37h GHz.	27
Figure 11: Same as Figure 6, but for SSMIS channel 91v GHz.....	29
Figure 12: Same as Figure 6, but for SSMIS channel 91h GHz.	31

List of Tables

Table 1: SSMIS FCDR instrument data availability at CM SAF.	9
Table 2: Requirement values for the SSMIS brightness temperatures product CM-12001 as given in the Product Requirements Document [AD 2].	16
Table 3: Statistics of the ensemble anomalies for SSMIS channel 19v GHz. The first block shows the original RDR with EIA normalized, the second block the CM SAF FCDR and the last block the CSU FCDR.	20
Table 4: Statistics of instrument differences for SSMIS channel 19v GHz. The numbers represent percentiles of absolute differences less than 1K, 2K, and 3K of all monthly mean grid boxes between two instruments.....	20
Table 5: Statistics of the ensemble anomalies for SSMIS channel 19h GHz. The first block shows the original RDR with EIA normalized, the second block the CM SAF FCDR and the last block the CSU FCDR.	22





 	EUMETSAT SAF on CLIMATE MONITORING Validation Report Microwave Radiance FCDR R2	Doc.No.: SAF/CM/DWD/VAL/FCDR_SSMIS Issue: 1.1 Date: 2015-02-26
---	--	--

Table 6: Statistics of instrument differences for SSMIS channel 19h GHz. The numbers represent percentiles of absolute differences less than 1K, 2K, and 3K of all monthly mean grid boxes between two instruments.....	22
Table 7: Statistics of the ensemble anomalies for SSMIS channel 22v GHz. The first block shows the original RDR with EIA normalized, the second block the CM SAF FCDR and the last block the CSU FCDR.	24
Table 8: Statistics of instrument differences for SSMIS channel 22v GHz. The numbers represent percentiles of absolute differences less than 1K, 2K, and 3K of all monthly mean grid boxes between two instruments.....	24
Table 9: Statistics of the ensemble anomalies for SSMIS channel 37v GHz. The first block shows the original RDR with EIA normalized, the second block the CM SAF FCDR and the last block the CSU FCDR.	26
Table 10: Statistics of instrument differences for SSMIS channel 37v GHz. The numbers represent percentiles of absolute differences less than 1K, 2K, and 3K of all monthly mean grid boxes between two instruments.....	26
Table 11: Statistics of the ensemble anomalies for SSMIS channel 37h GHz. The first block shows the original RDR with EIA normalized, the second block the CM SAF FCDR and the last block the CSU FCDR.	28
Table 12: Statistics of instrument differences for SSMIS channel 37h GHz. The numbers represent percentiles of absolute differences less than 1K, 2K, and 3K of all monthly mean grid boxes between two instruments.....	28
Table 13: Statistics of the ensemble anomalies for SSMIS channel 91v GHz. The first block shows the original RDR with EIA normalized, the second block the CM SAF FCDR and the last block the CSU FCDR.	30
Table 14: Statistics of instrument differences for SSMIS channel 91v GHz. The numbers represent percentiles of absolute differences less than 1K, 2K, and 3K of all monthly mean grid boxes between two instruments.....	30
Table 15: Statistics of the ensemble anomalies for SSMIS channel 91h GHz. The first block shows the original RDR with EIA normalized, the second block the CM SAF FCDR and the last block the CSU FCDR.	32
Table 16: Statistics of instrument differences for SSMIS channel 91h GHz. The numbers represent percentiles of absolute differences less than 1K, 2K, and 3K of all monthly mean grid boxes between two instruments.....	32

 	EUMETSAT SAF on CLIMATE MONITORING Validation Report Microwave Radiance FCDR R2	Doc.No.: SAF/CM/DWD/VAL/FCDR_SSMIS Issue: 1.1 Date: 2015-02-26
---	--	--

I Preface

I-1 The EUMETSAT SAF on Climate Monitoring

The importance of climate monitoring with satellites was recognized in 2000 by EUMETSAT Member States when they amended the EUMETSAT Convention to affirm that the EUMETSAT mandate is also to “contribute to the operational monitoring of the climate and the detection of global climatic changes”. Following this, EUMETSAT established within its Satellite Application Facility (SAF) network a dedicated centre, the SAF on Climate Monitoring (CM SAF, <http://www.cmsaf.eu/>).

The consortium of CM SAF currently comprises the Deutscher Wetterdienst (DWD) as host institute, and the partners from the Royal Meteorological Institute of Belgium (RMIB), the Finnish Meteorological Institute (FMI), the Royal Meteorological Institute of the Netherlands (KNMI), the Swedish Meteorological and Hydrological Institute (SMHI), the Meteorological Service of Switzerland (MeteoSwiss), and the Meteorological Service of the United Kingdom (UK MetOffice). Since the beginning in 1999, the EUMETSAT Satellite Application Facility on Climate Monitoring (CM SAF) has developed and will continue to develop capabilities for a sustained generation and provision of Climate Data Records (CDR's) derived from operational meteorological satellites.

In particular the generation of long-term data sets is pursued. The ultimate aim is to make the resulting data sets suitable for the analysis of climate variability and potentially the detection of climate trends. CM SAF works in close collaboration with the EUMETSAT Central Facility and liaises with other satellite operators to advance the availability, quality and usability of Fundamental Climate Data Records (FCDRs) as defined by the Global Climate Observing System (GCOS). As a major task the CM SAF utilizes FCDRs to produce records of Essential Climate Variables (ECVs) as defined by GCOS. Thematically, the focus of CM SAF is on ECVs associated with the global energy and water cycle.


The CM SAF data sets can serve applications related to the new Global Framework of Climate Services initiated by the WMO World Climate Conference-3 in 2009. CM SAF is supporting climate services at national meteorological and hydrological services (NMHSs) with long-term data records but also with data sets produced close to real time that can be used to prepare monthly/annual updates of the state of the climate. Both types of products together allow for a consistent description of mean values, anomalies, variability, and potential trends for the chosen ECVs. CM SAF ECV data sets also serve the improvement of climate models both at global and regional scale.

A catalogue of all available CM SAF products is accessible via the CM SAF webpage, <http://www.cmsaf.eu/>. Here, detailed information about product ordering, add-on tools, sample programs and documentation is provided.

I-2 Introduction

This CM SAF validation report provides information on the evaluation of the Fundamental Climate Data Record (FCDR) of Microwave Brightness Temperatures from the Special Sensor Microwave/Imager (SSM/I) and the Special Sensor Microwave Imager/Sounder (SSMIS). The SSMIS data record is a continuation of the SSM/I FCDR (available from CM SAF; http://dx.doi.org/10.5676/EUM_SAF_CM/FCDR_SSMI/V001) and both are integral parts of this second release.

The predecessors of this data record and the data processor suite have originally been developed at the Max-Planck Institute for Meteorology (MPI-M) and the University of Hamburg (UHH) for the

	EUMETSAT SAF on CLIMATE MONITORING Validation Report Microwave Radiance FCDR R2	Doc.No.: SAF/CM/DWD/VAL/FCDR_SSMIS Issue: 1.1 Date: 2015-02-26
---	--	--

Hamburg Ocean Atmosphere Parameters and Fluxes from Satellite Data (HOAPS, <http://www.hoaps.org/>) climatology. HOAPS is a compilation of climate data records for analysing the water cycle components over the global oceans derived from satellite observation (Andersson et al. 2011). The main satellite instrument employed to retrieve the geophysical parameters is the SSM/I and much work has been invested to process and carefully homogenize all SSM/I instruments onboard the Defence Meteorological Satellite Program (DMSP) platforms F08, F10, F11, F13, F14 and F15 (Andersson et al. 2010).

In order to derive reliable long term trend estimates of the global water cycle parameters it is strictly necessary to carefully correct for all known problems and deficiencies of the SSM/I radiometers as well as to inter-calibrate and homogenise the different instruments. Moreover, all applied corrections need to be clearly documented to provide a complete calibration traceability for a Fundamental Climate Data Record (FCDR). Following these recommendations, CM SAF released a FCDR of SSM/I brightness temperatures in 2013, freely available from the web user interface (<http://wui.cmsaf.eu/>; (doi:10.5676/EUM_SAF_CM/FCDR_SSMI/V001)). This FCDR has already been used in the ESA CCI Sea ice project and will also be used in the upcoming reanalysis ERA5.

In order to further extend the HOAPS dataset in time, the SSM/I successor instrument SSMIS has to be used from 2009 onwards. CM SAF has now reprocessed the SSMIS sensors onboard F16, F17, and F18 to the same standards as the SSM/I data record for the time period 2006 - 2013. This FCDR is a completely reprocessed SSMIS data record, thus ensuring a maximum in homogeneity by applying a common processing scheme and inter-calibration model for all observations.

It is important to keep in mind that the SSMIS is a completely redesigned instrument and not just an extension of the SSM/I instrument series. It does provide a continuation of the basic SSM/I observed frequencies (19, 22, 37 GHz). However, it is not expected to give identical brightness temperatures per se. A combination of both data records with an inter-sensor calibration can thus be defined as a FCDR for a specific frequency, spanning the complete time period. Otherwise, also a sensor specific FCDR can be defined, providing consistent data records for one sensor type. This leads to the potential paradigm, that a FCDR can be defined in two ways:

- with a primary aim as the consistency across sensors with sensor calibration being a secondary consideration, or
- with a focus on accuracy on each sensor data record independently with consistency diagnosed rather than constraint.

In order to aim for one data set able to fulfil both paradigms, one important feature of this FCDR is the flexibility to use the same data record with or without inter-calibration. The brightness temperatures, corrected for instrument anomalies, and the inter-calibration offsets are provided as separate layers in one data file, allowing the users to individually choose whether to apply the correction (adding the offset) or not. In this sense, the first release of the Microwave Radiance FCDR (CM-150), covering the SSM/I and the newly generated SSMIS record form together the second release (CM-12001), defined as a combined FCDR with optimal sensor calibration and consistency.

II SSM/I

The SSM/I component of this combined FCDR remains unchanged compared to the first release and therefore also the corresponding documents ATBD [RD 3], Product User Manual [RD 4], and Validation Report [RD 5] are still applicable to the SSM/I data record part. These documents are available from www.cmsaf.eu/doc. The data records and the documents are also easily accessible from the SSM/I FCDR DOI summary webpage [http://dx.doi.org/10.5676/EUM_SAF_CM/FCDR_SSMI/V001].

III SSMIS

The CM SAF FCDR from SSMIS brightness temperatures is compiled as daily collections of all observations from each sensor. All sensor specific data available in the raw data records are provided as well as additional information like quality control flags, Earth incidence angles (EIA), averaged 91 GHz brightness temperatures, synthetic 85 GHz brightness temperatures, incidence angle normalisation offsets and inter-sensor calibration offsets. The SSMIS FCDR is available for the time period from November 2005 until December 2013. A detailed list of data availability for each of the three SSMIS platforms is given in Table 1.

A technical description of the data sets including information on the file format as well as on the data access is provided in the Product User Manual [RD 1]. Furthermore details on the CM SAF inter-sensor calibration model, the implementation of the processing chain and individual processing steps are available in the Algorithm Theoretical Basis Document [RD 2]. Basic accuracy requirements are defined in the product requirements document [AD 2]. An extensive description of the SSMIS instrument and satellite characteristics has been published by Kunkee et al. (2008).

III-1 Instrument and sensor stability

Figure 1 shows the time series of the mean DMSP platform local equator crossing times, altitude and the Earth Incidence Angles (EIA) of the different SSMIS instruments. The local overpass time is not constant for all platforms. The strongest drift can be observed for F16 from 8 to 5 AM/PM while F17 and F18 show a more constant equator crossing time at 6 and 8 AM/PM, respectively. Due to the drift in overpass time, the brightness temperature (TB) differences between the instruments are not constant and the diurnal cycle variation must be taken into account when comparing the inter satellite differences.

The altitude of the satellite platforms is very constant over time, as depicted in the Figure 1, middle panel. Therefore, also the orbit mean EIA remains constant. However, due to varying alignments of the feedhorns on the different platforms, the mean EIA ranges between 52.9 to 53.3 degrees (Figure 1, lower panel). The variation of the local EIA at equator crossing is caused by the orbit precession and can also lead to differences up to 0.2 degree in EIA. Since a change of 0.1 degree in EIA will change the vertical polarized TB up to 0.2 K, these variations must be taken into account by normalizing the observed TBs to a constant EIA. The CM SAF FCDR data files contain offsets, which are computed using the Furhop and Simmer (1996) algorithm to normalize the TBs to 53 degree EIA.

Figure 2 shows the time series of the hot load target temperatures and the reflector arm temperatures for all instruments. The temperature of the warm calibration target is very constant at about 310 K. This is a clear improvement over the SSM/I design, where a strong seasonal variability with an amplitude of up to 50 K was observed. The variation in the arm temperature is an important indicator for the correction of the reflector emissivity problem. It depends on the amount of time spent in the Earth shadow during an orbit and thus on the local equator overpass time. This dependency can be observed from the change in the seasonal arm temperature variations of F16, when the overpass time drifts from 8 to 6 AM/PM. In the beginning the seasonal variation in warm

Table 1: SSMIS FCDR instrument data availability at CM SAF.

DMSP platform	Launch date	Record start	Record end
F16	2003-10-08	2005-11-01	2013-12-31
F17	2006-11-04	2006-12-14	2013-12-31
F18	2009-10-18	2010-03-08	2013-12-31

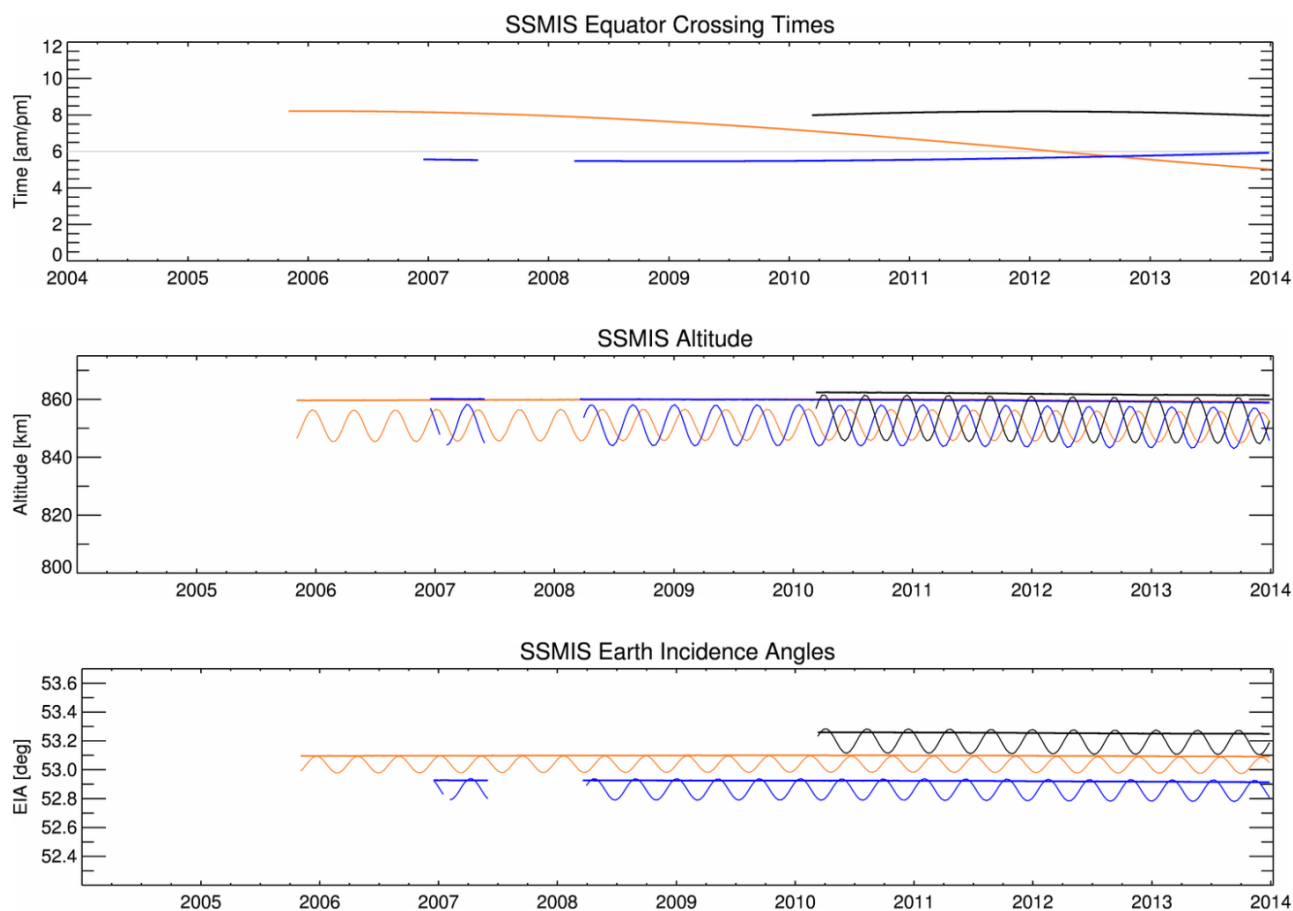


Figure 1: Time series of DMSP platform mean local equator crossing times, altitude and the Earth Incidence Angles of the different SSMIS instruments. Thin lines are the mean values at the ascending equator crossing and thick lines depict complete orbit mean values. Colours are as follows: F16 orange, F17 blue, F18 black.

target temperature is very small, but starts to undergo strong cooling events from 2015 onward when the local overpass time has drifted before 7 AM/PM. The minima in the arm temperatures are occurring at solar equinox in spring and autumn. When F17 and F16 are at the same overpass time, the seasonal arm temperature variations are nearly identical.

Figure 3 shows the time series of the radiometer sensitivities for all SSM/I-like channels. This radiometer noise is estimated at the warm calibration target temperature and archived in the CM SAF FCDR data files. Overall, the radiometer noise is within the specification for most of the channels. The most pronounced feature is an increase in the noise for the F18 in early 2012 in all channels with a maximum increase in the 37h channel from 0.4 K to 0.8 K. The most problematic channel is the 91h onboard F16. It is above the specification and depicts a very noisy behaviour.

III-2 Evaluation of Brightness Temperature differences

The purpose of a validation is to establish that the measurement under scrutiny agrees with an independent, and (ideally) traceable, measurement or estimate, within the combined measurement uncertainties in both. A conclusion from the error budget estimation (see ATBD [RD 2]) is that a complete comprehensive validation of the SSM/I / SSMIS brightness temperatures is not possible, as there is no absolute validation reference available. The final aim of an evaluation process must be to show that the measured SSM/I brightness temperatures are in agreement with modelled brightness temperatures within the expected random uncertainties. As a major requisite, a

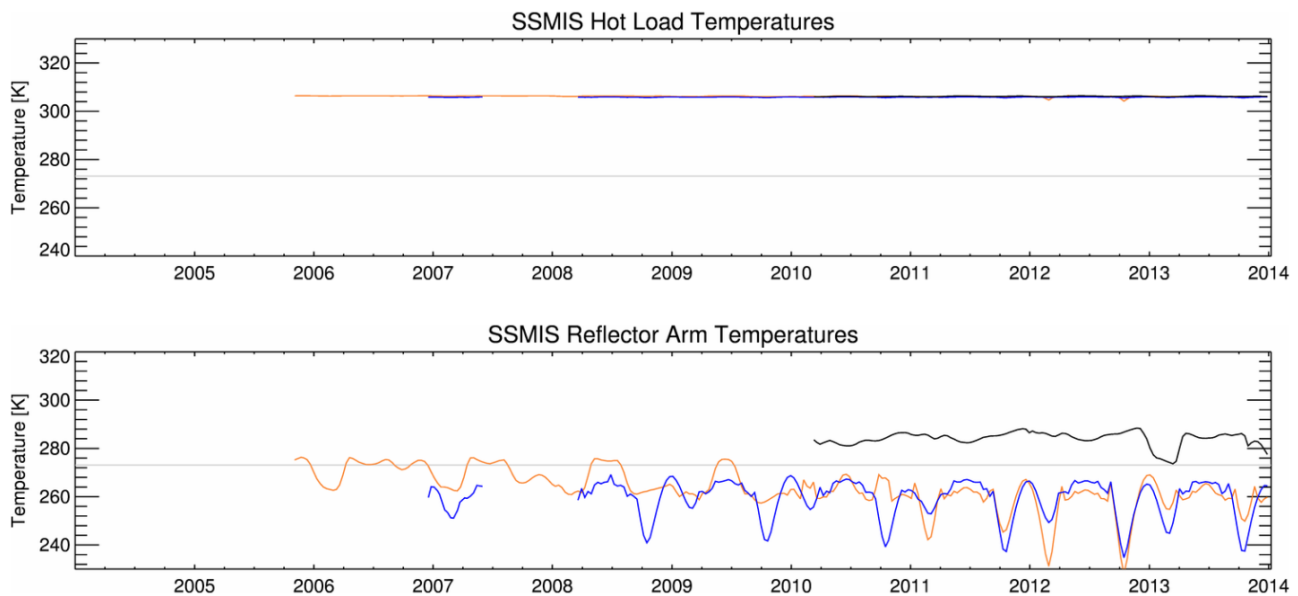


Figure 2: Time series of SSMIS sensor diagnostics: Temperature of the warm calibration target (upper panel) and temperature of the reflector arm (lower panel). The grey lines denote 0°C (for colours see Figure 1).

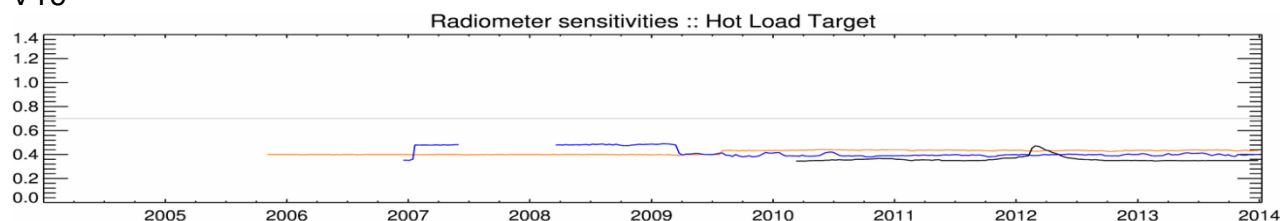
Fundamental Climate Data Record must show improved quality compared to the existing Raw Data Records (RDR) in order to be a useful data set, providing added value to the user community.

Hence, the validation strategy in this document is to compare this FCDR of SSMIS brightness temperatures to the original RDR and to the CSU SSMIS FCDR (Berg, 2013), in order to quantify the quality of the inter-sensor calibration (see ATBD [RD 2])) and to compare the different inter-sensor calibration approaches. The aim of this validation report is to show that the homogeneity of the reprocessed FCDR is significantly improved compared to the original raw Temperature Data Records.

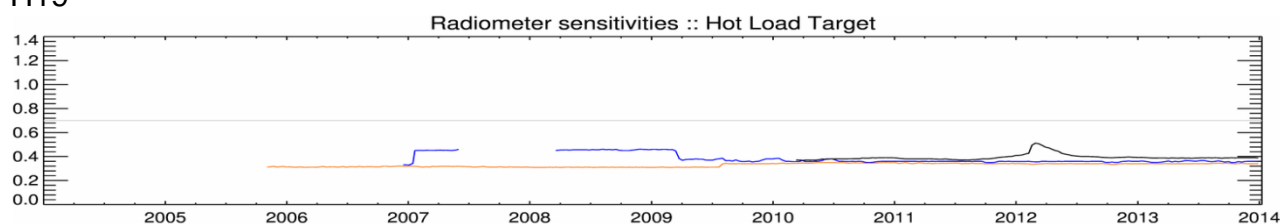
III-2.1 Data Sets for Comparison

Another FCDR of SSMIS brightness temperature has been released from Colorado State University (CSU). The inter-sensor calibration model used for this data set is described in detail in Sapiano and Berg (2013) and Berg and Sapiano (2012). The CSU inter-calibration model uses the F13 as reference instrument. The inter-calibration is implemented in a two step process. First a matchup database against rain-free TMI observation over ocean is used to correct for solar intrusion effects. This data base consists of double differences (SSMIS-model)-(TMI-model) as a function of solar azimuth, solar elevation, and scene temperature. After this correction to TMI has been applied, the SSMIS TBs are inter-calibrated to the F13 using the mean of different types of double differences. The scene dependence is solved via a look-up table with tie-points. For TBs outside the covered range, the maximum and minimum values are applied respectively.

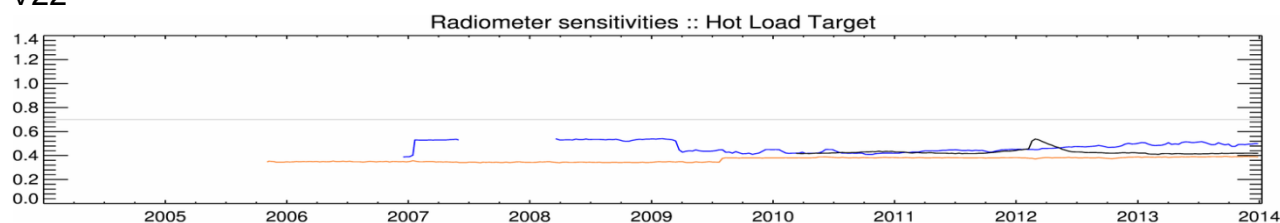
V19



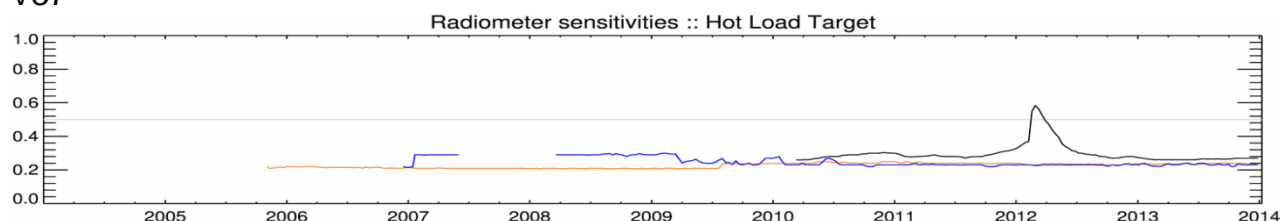
H19



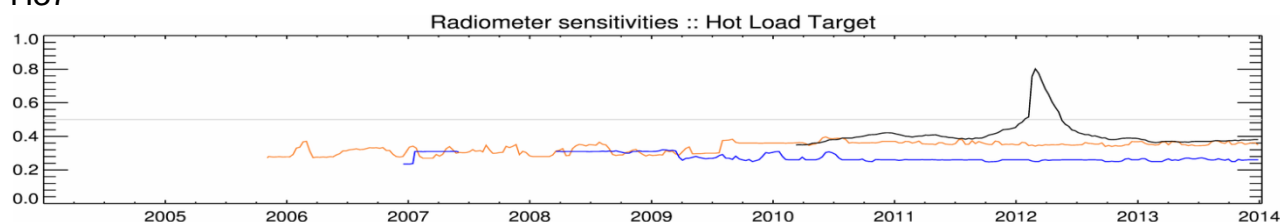
V22



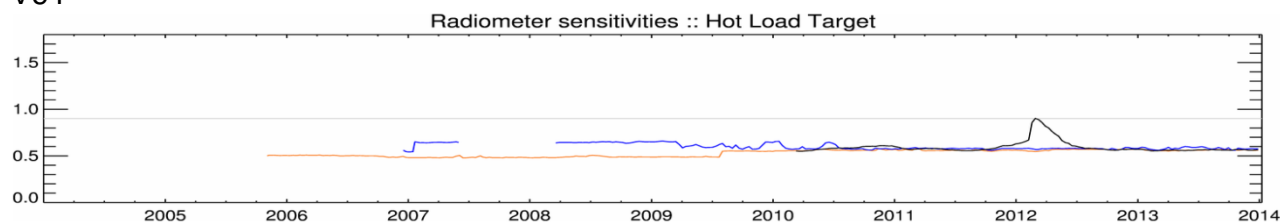
V37



H37



V91



H91

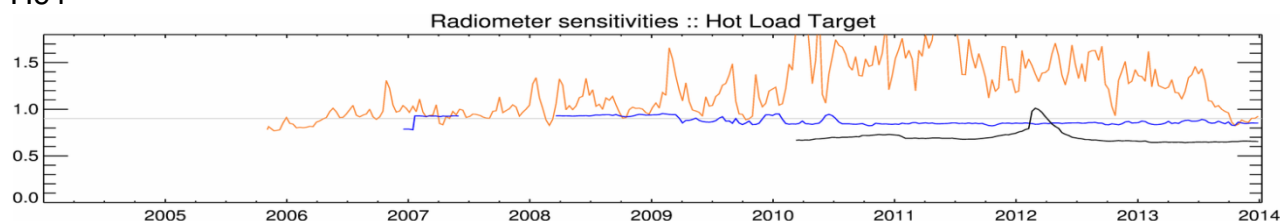




Figure 3: Time series of SSMIS sensor diagnostics: Radiometer sensitivities for the channels at 19v, 19h, 22v, 37v, 37h, 91v and 91h GHz. The grey lines denote the specification values for colours see Figure 1).

 	EUMETSAT SAF on CLIMATE MONITORING Validation Report Microwave Radiance FCDR R2	Doc.No.: SAF/CM/DWD/VAL/FCDR_SSMIS Issue: 1.1 Date: 2015-02-26
---	--	--

III-2.2 Visual inspection

Before evaluating the TB differences statistically, a visual inspection of brightness temperature differences for all satellite pairs has been done to test the performance of the inter-sensor calibration models over all surface types. The warmest TBs over land are not used directly during the inter-calibration model fitting procedure of the CM SAF FCDR due to the strong diurnal cycle of the land surface. As the overpass time between the satellites differs by up to two hours, significant differences in the brightness temperature are to be expected over land surfaces. The main challenge for the inter-calibration model is to keep the natural variability unchanged but to only correct for instrument biases. However, the mean diurnal variability over land is assumed to be independent of the polarization at a given frequency. Thus, double differencing $((TB_{v_{S1}} - TB_{v_{S2}}) - (TB_{h_{S1}} - TB_{h_{S2}}))$ can be used to remove the diurnal effects and no residual biases should remain for the inter-calibrated sensors. As the result of these comparisons, two examples are presented in Figure 4 and Figure 5. The figures show the climatological daily mean (AM and PM) of TB differences at 19 GHz between F13 and F16 (Figure 4) and between F17 and F18 (Figure 5). The first example is of major importance, because F16 is defined as the transfer target from the SSM/I to the SSMIS era.

The uncorrected raw data (Figure 4, left column) show a strong scene dependent bias between F13 and F16. The overpass time difference between the satellites is about 2 hours. Therefore negative anomalies due to the diurnal cycle should be clearly visible over land areas for the vertical and horizontal polarization, while no significant difference over the ocean is expected. However, these anticipated features are not depicted in the uncorrected data. The FCDRs from CM SAF (middle column) as well as from CSU (right column) both remove the observed inter-sensor differences over the oceans. The remaining anomalies in the CM SAF FCDR show small negative values over the northern oceanic areas and small positive values for the southern oceans. Vertical and horizontal polarizations depict, as expected, a similar diurnal pattern after correction and no significant residual biases appear in the double difference plot (middle column, bottom panel). The CM SAF FCDR also shows small biases over the Sahara desert and Greenland, which are due to missing incidence angle corrections for these surface types. The large differences over Antarctica are caused by the gridding procedure and are artificial.

However, for the CSU FCDR very strong differences remain in the double difference image over land surfaces and sea-ice (right column, bottom panel). In this case, the inter-calibration procedure completely removes the natural diurnal signal over land from the 19v channel (right column, top panel). Positive anomalies remain for the 19h channel (right column, middle panel), whereas negative anomalies are to be expected due to the diurnal warming of the land surface. Also, a precipitation pattern is visible in the difference of the channel 19h. This observed bias is most likely caused by an underestimation of the scene dependence. The CSU inter-calibration coefficients are determined over the TRMM covered area ($\pm 40^\circ$ latitude), using only rain-free observation over ocean. This limits the utilized spectrum to the radiometric cold end while excluding all radiometric warm targets and thus existing scene dependences are not recognised.

Figure 5 shows the differences between F17 and F18 for the 19 GHz channels. The overpass time difference is less than for F13/F16 and thus the residual warm biases over land are consistently smaller in the CM SAF FCDR. As for the comparison of F13 and F16, the CSU FCDR does not depict such a consistent behaviour. The differences for the horizontal polarization (right column, middle panel) over land are considerable larger than for the vertical polarization (right column, top panel). This leads to a significant positive residual bias over radiometric warm surfaces (sea ice, land) in the comparison of F17 and F18 (right column, bottom panel). Both FCDRs perform well over ocean and remove the observed differences.

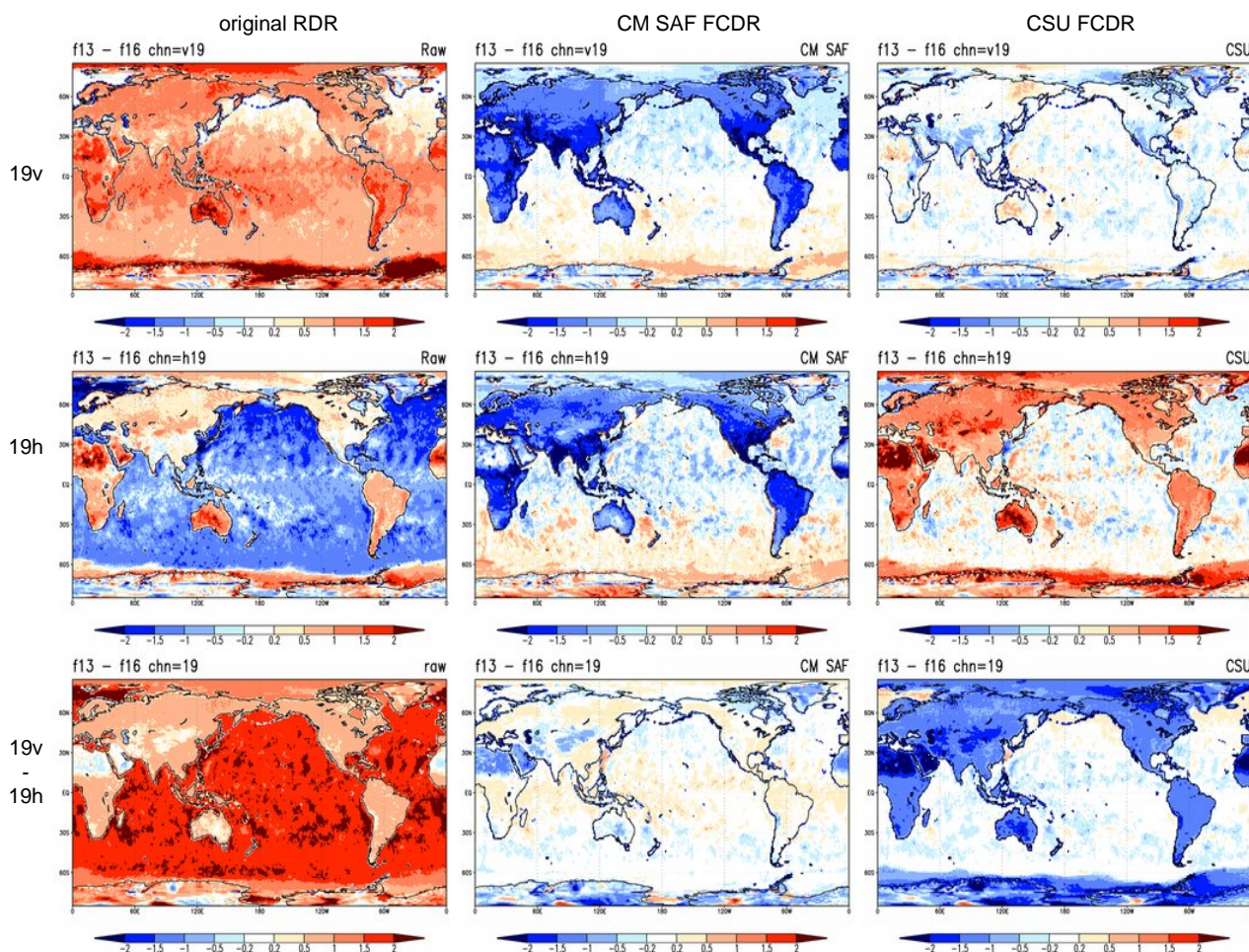


Figure 4: Climatological mean of TB differences at 19 GHz between SSM/I F13 and SSMIS F16. The left column shows the original uncorrected raw data records. The middle column depicts the CM SAF FCDR and the right column shows the CSU FCDR. The top row shows the vertical polarisation, the middle row the horizontal polarisation and the bottom row depicts the double differences between both polarisations.

The other difference maps for channels and instrument pairs not presented here, show similar results but with increasing noise at higher frequencies. All comparison maps are collected in a separate document, available from the CM SAF website at http://www.cmsaf.eu/validation_report/.

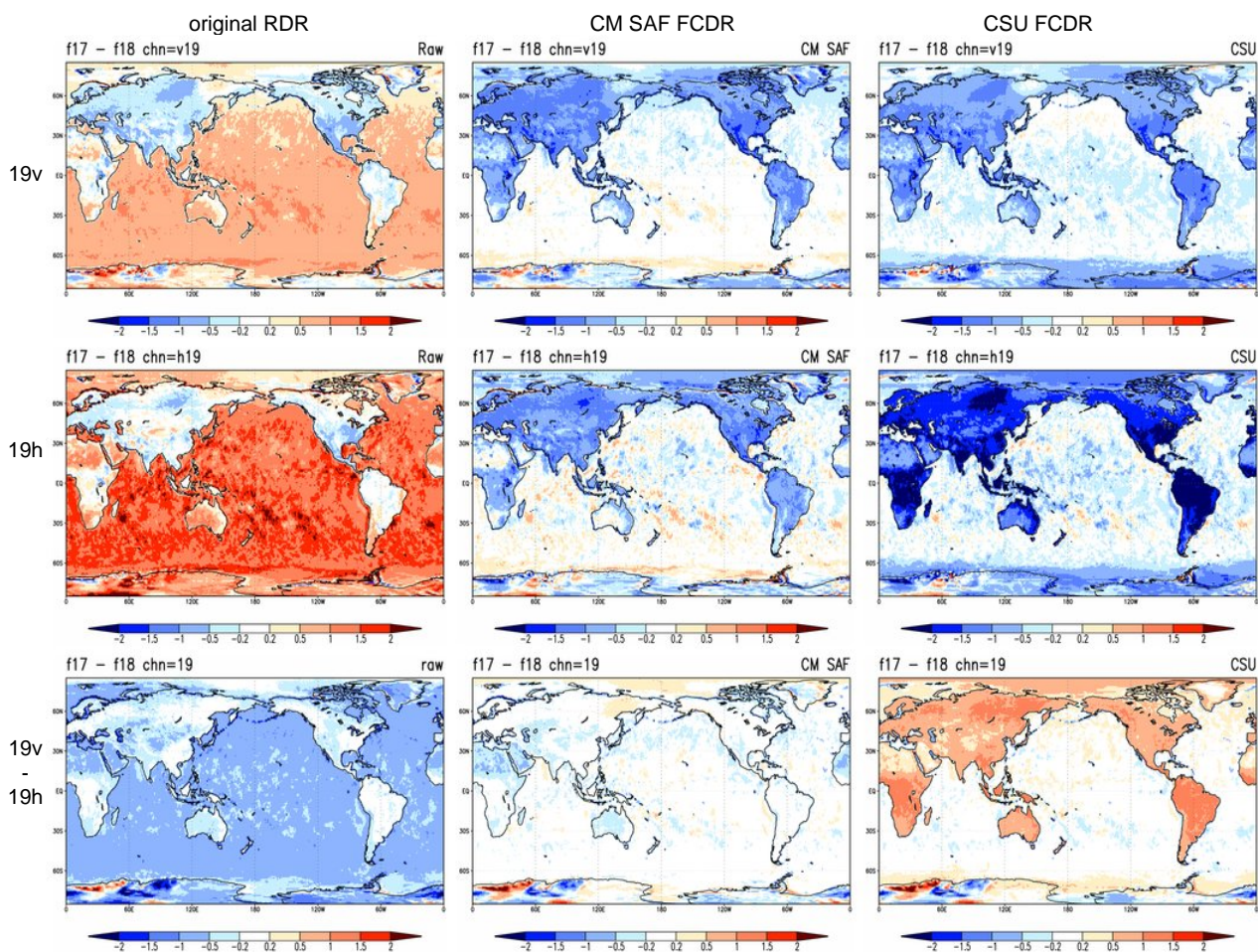




Figure 5: As Figure 4 but for the SSMIS TB differences at 19 GHz between F17 and F18.

III-2.3 Evaluation strategy

Similar to the visual inspection, the CM SAF FCDR is compared to the RDR and CSU brightness temperature data set. The homogeneity of the data sets is tested by comparing against the respective ensemble mean of the available satellites in each data record and additional statistical values are given for bias, robust standard deviation (RSD), median absolute deviation (MAD) and decadal stability. The requirements for the SSMIS brightness temperature product are defined in the Product Requirements Document (PRD) [AD 2]. Table 2 lists the relevant statistical measures for monthly global mean values.

In order to quantify the consistency of the brightness temperatures across the SSMIS sensors, a reference has to be established first. As there is no absolute reference available and the operating sensors change over time, we choose the ensemble mean of all available instruments at each month as the relative reference. This approach simplifies the further analysis, as it can be performed per sensor and not for all sensor pairs. The inter-sensor differences are derived by comparing the respective bias values to the ensemble mean. The maximum inter-sensor difference is the ensemble spread, which characterizes the observation uncertainty, because without additional information each sensor could be treated as the “true” observation.

A global monthly mean bias only characterizes the mean systematic offset to another sensor. However, it is also important to quantify the observed regional differences, which is characterized by the distribution of gridded monthly mean brightness temperature differences. The median of

 	EUMETSAT SAF on CLIMATE MONITORING Validation Report Microwave Radiance FCDR R2	Doc.No.: SAF/CM/DWD/VAL/FCDR_SSMIS Issue: 1.1 Date: 2015-02-26
---	--	--

absolute differences (MAD), without correcting for the mean systematic offset (bias), is a measure of the total absolute uncertainty. In terms of monthly mean gridded data samples, a MAD of 1 K means that 50% of all grid box brightness temperature differences are within 0-1 K. A robust (resilient to outliers) measure of the statistical dispersion of a distribution is the median absolute deviation about the median. Assuming a normal distribution, the expected standard deviation can be estimated from the median absolute deviation by scaling it with a factor of 1.48. For comparison this approach has also been applied to the CSU data set which covers the same time period as the CM SAF FCDR. Prior to consistency analysis the data files have first been converted to the CM SAF data format. Then both data sets have been gridded to equal angle 1° monthly mean global fields separately for AM and PM orbits. For the comparisons all oceanic and sea-ice covered grid cells are used.

To evaluate the relative instrument differences, an ensemble mean data set has been compiled for each FCDR on a monthly basis for all instruments and channels. The ensemble monthly mean grid box brightness temperature $\langle T_B \rangle$ for each month t and grid box index g is calculated as the arithmetic mean of the individually gridded monthly mean brightness temperatures T_B from all available instruments s :

$$\langle T_B \rangle(t, g) = \frac{1}{N_s} \cdot \sum_{s=1}^{N_s} T_B(s, t, g), \quad (1)$$

with N_s as the number of contributing instruments for each grid box and month.

The distribution of brightness temperature differences ΔT_B relative to this ensemble mean

$$\Delta T_B(s, t, g) = T_B(s, t, g) - \langle T_B \rangle(t, g) \quad (2)$$

is then statistically analysed. Here we apply robust statistics (see above), with M as the median of the distribution of all grid box brightness temperature differences ΔT_B for each instrument s . We define:

$$\begin{aligned} Bias_s &= M(\Delta T_B(t, g)|_s) \\ MAD_s &= M(|\Delta T_B(t, g)|_s) \\ RSD_s &= M(|Bias_s - \Delta T_B(t, g)|_s) \cdot 1.48 \end{aligned} \quad (3)$$

The requirement for the global monthly mean consistency between the instruments is given in Table 2 in terms of inter-sensor biases. As $Bias_s$ is relative to the ensemble mean, the inter-sensor bias is derived as the corresponding difference $Bias_{s1} - Bias_{s2}$.



The decadal stability t_D for each channel and instrument is estimated using a linear model trend, fitted to the time series of monthly anomalies relative to the ensemble mean. The anomalies are defined as the median of the global distribution of brightness temperature differences ΔT_B :

$$\overline{\Delta T_{B,s}}(t) = M[\Delta T_B(g)|_s](t). \quad (4)$$

A simple model with a linear decadal trend t_D in K/decade is then defined as:

Table 2: Requirement values for the SSMIS brightness temperatures product CM-12001 as given in the Product Requirements Document [AD 2].

	Threshold	Target	Optimal
Bias	3K	2K	1K
Decadal stability $t_D = 0.03$ K/decade	Significance $\alpha \geq 0.3\%$	Significance $\alpha \geq 5\%$	Significance $\alpha \geq 30\%$



 	EUMETSAT SAF on CLIMATE MONITORING Validation Report Microwave Radiance FCDR R2	Doc.No.: SAF/CM/DWD/VAL/FCDR_SSMIS Issue: 1.1 Date: 2015-02-26
---	--	--

$$\overline{\Delta T_{B,s}}(t) = \overline{\Delta T_{B,s}}(t = 0) + \frac{t_D}{120} \cdot t + \varepsilon(t), \quad (5)$$

with $\varepsilon(t)$ representing the fraction of the monthly anomalies not explained by the linear approximation. The linear model terms (offset and trend) are found by a least square regression fit. The stability requirement, as defined in the requirement review (Table 2), is a decadal stability with a linear trend of $t_D < 0.03 \text{ K/decade}$. The requirement levels are defined in terms of significance levels of statistical hypothesis testing. The null hypothesis $t_D > 0.03 \text{ K/decade}$ can be rejected (criterion is met) if the probability of rejecting the null hypothesis is higher than the threshold (0.3%), target (5%) or optimal (30%) criterion (see Table 2). The significance level α of the decadal trend is determined using a two-sided t-test, assuming a standard uncertainty of 0.1 K for the distribution of the global monthly anomalies $\overline{\Delta T_{B,s}}(t)$.

The results of the statistical analysis are shown in Figure 6 to Figure 12 and summarized in Table 3 to Table 16, grouped by channel. The tables also contain the maximum inter-sensor bias which is simply the maximum of all bias differences computed using the first equation in Eq. (3). All figure panels contain 5 images with time series of monthly mean values of:

1. TB anomalies of the raw data record,
2. TB anomalies after EIA normalization and diurnal cycle removed,
3. TB anomalies of the CM SAF FCDR,
4. TB anomalies of the CSU FCDR,
5. Robust standard deviation (RSD) of CM SAF FCDR TB anomalies.

 	EUMETSAT SAF on CLIMATE MONITORING Validation Report Microwave Radiance FCDR R2	Doc.No.: SAF/CM/DWD/VAL/FCDR_SSMIS Issue: 1.1 Date: 2015-02-26
---	--	--

III-2.4 Evaluation Results

The time series of the raw data records plots (RDR, Figure 6 to Figure 12 top panel) show a very diverse picture. The agreement in the raw data record between the SSM/I is generally better than between the SSMIS. This is also evident for the homogenised data records that have been corrected for incidence angle and diurnal cycle variations (RDR, Figure 6 to Figure 12 second panel). The largest differences for the SSM/I is 1K in the 37 GHz channel. In contrast to this, most of SSMIS differences are around 1 K before the inter-calibration. The ensemble spread between SSM/I and SSMIS channels are larger than 3K in the 37 GHz channels. Best agreement between both sensor types is found for the 19 GHz channels with about 1K difference. This means, most of the observed differences before applying the inter-calibration offsets are larger than the estimated standard uncertainty of the SSM/I instrument, which is about 0.6 to 1 K (see ATBD [RD 2]).

Obviously the calibration and inter-calibration increases the quality and stability of the SSMIS data. The global climatological mean bias of the SSMIS has been reduced to below 0.05 K. As for the raw data record, the agreement in the FCDRs between the SSM/I is generally better than between the SSMIS.

Further results are summarised as follows:

- Both analysed FCDRs significantly reduce the observed differences between the monthly means and show very similar results for individual satellites. All global monthly mean inter-sensor differences are within the optimum requirement of 1K. In terms of maximum inter-sensor bias (ensemble spread), the CM SAF FCDR is performing slightly better. Comparing the absolute maximum difference between the individual satellite biases to the ensemble mean, the CM SAF FCDR shows a remaining ensemble spread between 0.05 to 0.15 K, while for the CSU FCDR values between 0.15 to 0.33 K remain.
- Overall, the monthly anomalies show a variability which is larger for horizontally polarized channels and increases with higher frequencies. This variability is caused by the inclusion of all scenes, i.e. no rain filtering is applied. This additional noise can be interpreted as an additional uncertainty due to differences in space and time collocation and sampling variability.
- For most of the channels, no significant trend can be observed. Only the 19v and 37v GHz channels show a trend above the threshold criteria for F18. However, the F18 time series is very short and seasonal variations still have an impact on decadal stability estimates. The applied t-test assumes a Gaussian distribution of independent observations, but anomalies affected by a remaining seasonal cycle, e.g. due to solar instrument heating or cooling, are not randomly distributed. The number of independent observations, especially for the short temporal coverage of only 4 years in case of F18, thus limits the relevance of a decadal stability estimate.
- The robust standard deviations show very constant values over time for all channels and satellites between 0.5K and 1K, which means, that about 70% of all analysed monthly mean grid boxes are within $\pm 0.5K$ to $\pm 1K$, respectively. The outliers above 1 K are caused by incomplete months and therefore increased variability due to a shorter sampling period.
- The RSD is slightly increased during the SSM/I and SSMIS overlap, but not significantly different.
- The statistical measures derived from both FCDRs depict a very good and similar performance of both data sets in terms of RSD and MAD. However, some channels (19v, 19h) in the CSU FCDR show a small remaining bias of about 0.2-0.3K.
- In the majority of cases F18 exhibits the largest noise level.

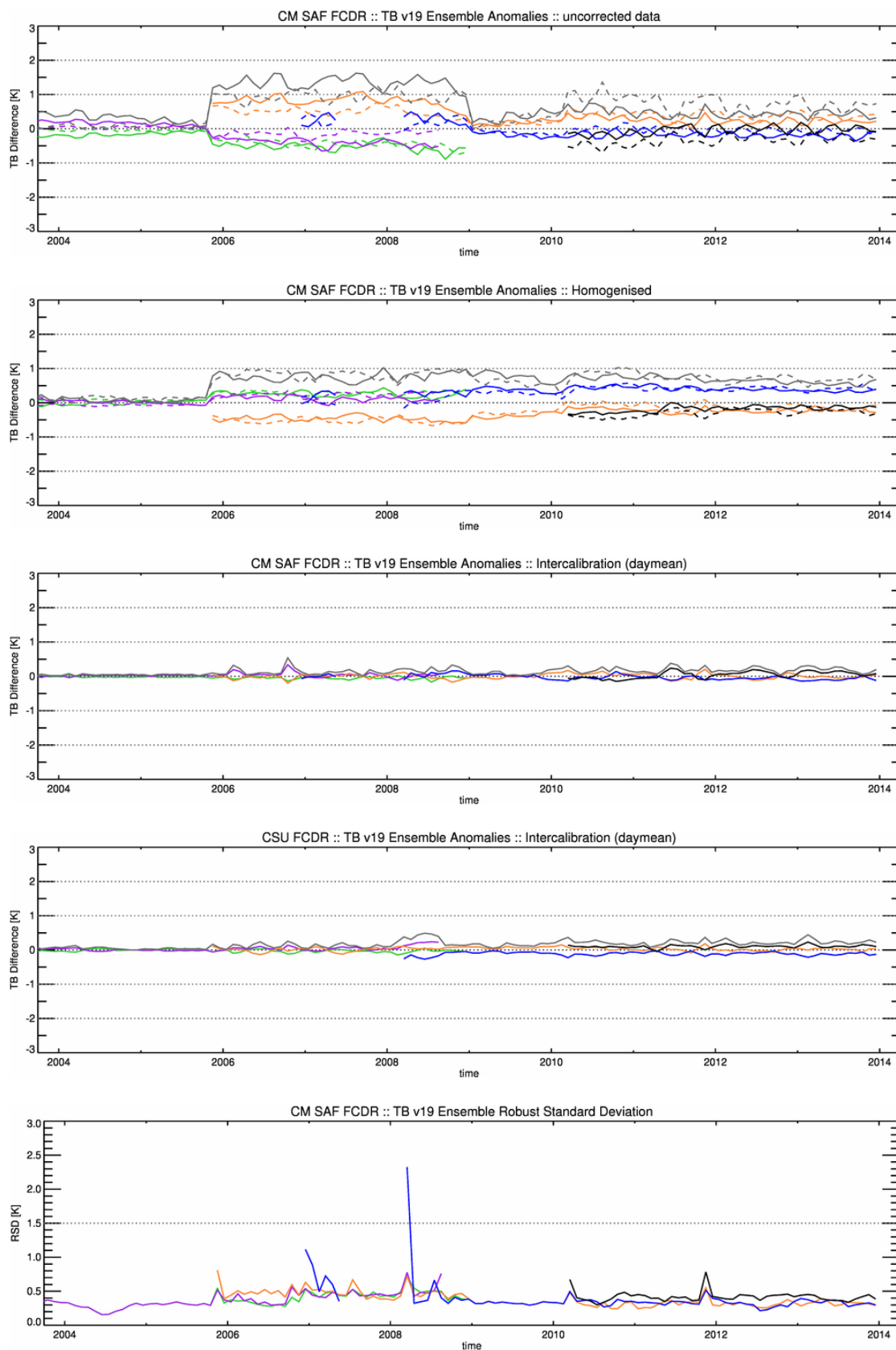


Figure 6: Time series of ensemble anomalies and variability for SSM/I & SSMIS channel 19v GHz. In the upper two panels the solid lines are PM orbits and the dashed lines AM orbits. The lower panels depict daily means of AM and PM orbits. The gray lines depict the ensemble spread. Horizontal dotted grey lines denote the optimal and target bias. For a detailed description see text (section III-2.3). Colours are as in Figure1 plus green (F13) and purple (F14).

Table 3: Statistics of the ensemble anomalies for SSMIS channel 19v GHz. The first block shows the original RDR with EIA normalized, the second block the CM SAF FCDR and the last block the CSU FCDR.

	F16	F17	F18
Bias [K]	- 0. 30	0. 36	- 0. 24
RSD [K]	0. 41	0. 36	0. 43
MAD [K]	0. 36	0. 41	0. 35
max absolute inter-sensor Bias [K]	0. 66	0. 66	0. 60
Bias [K]	- 0. 00	0. 03	0. 05
RSD [K]	0. 37	0. 35	0. 40
MAD [K]	0. 25	0. 24	0. 28
max absolute inter-sensor Bias [K]	0. 05	0. 03	0. 05
Trend [K/dec]	0. 09 ($\alpha > 30\%$)	- 0. 19 ($\alpha > 5\%$)	0. 50 ($\alpha < 0. 05\%$)
Bias [K]	0. 03	- 0. 11	0. 10
RSD [K]	0. 34	0. 34	0. 37
MAD [K]	0. 23	0. 25	0. 26
max absolute inter-sensor Bias [K]	0. 14	0. 21	0. 21

Table 4: Statistics of instrument differences for SSMIS channel 19v GHz. The numbers represent percentiles of absolute differences less than 1K, 2K, and 3K of all monthly mean grid boxes between two instruments.

	F16	F17	F18
F13	78. 1 95. 2 98. 7	69. 8 89. 3 95. 3	
F14	75. 9 94. 3 98. 4	66. 9 87. 1 94. 0	
F16		83. 5 96. 1 98. 7	83. 3 97. 0 99. 3
F17			82. 0 96. 7 99. 2

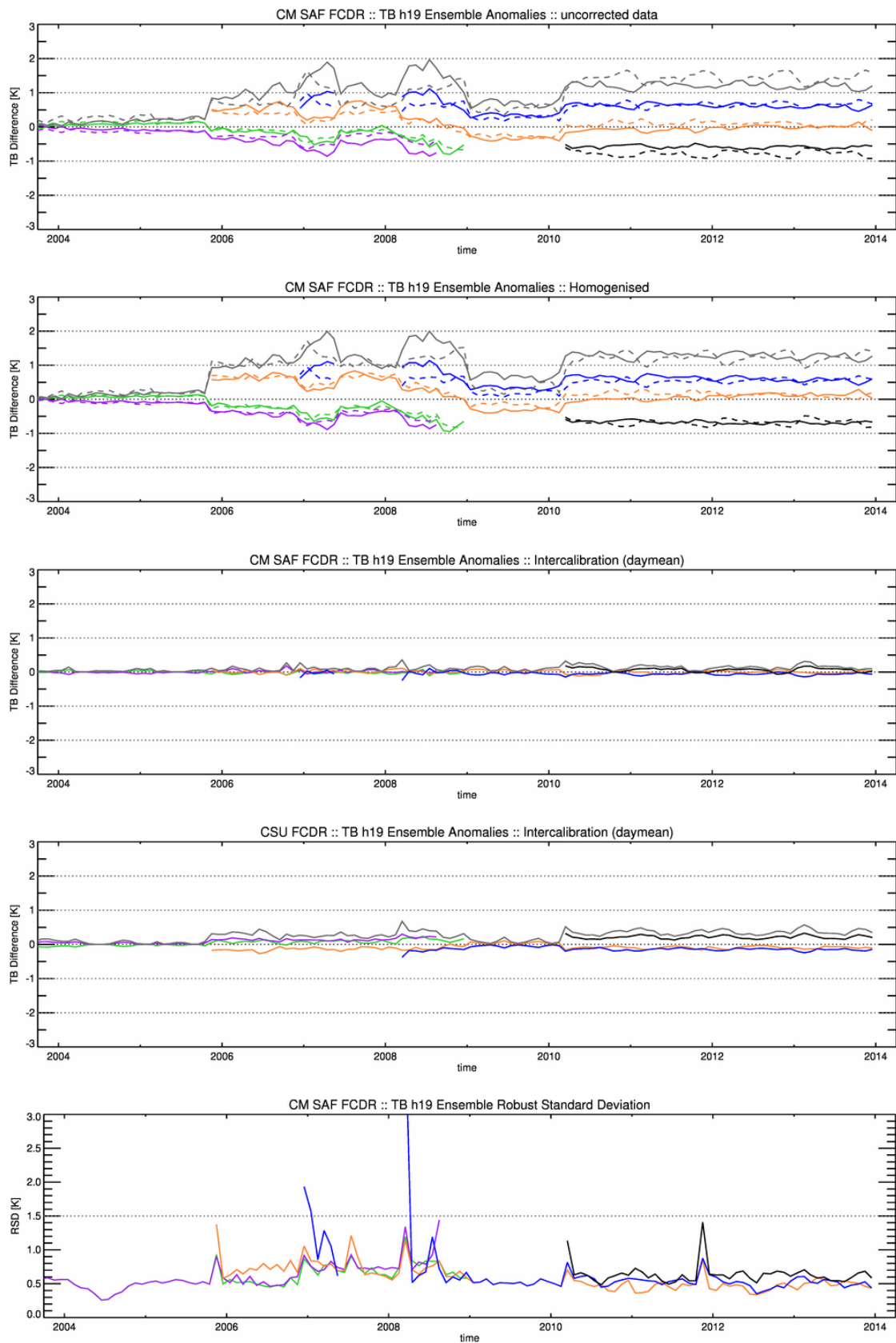


Figure 7: Same as Figure 6, but for SSM/I & SSMIS channel 19h GHz.

Table 5: Statistics of the ensemble anomalies for SSMIS channel 19h GHz. The first block shows the original RDR with EIA normalized, the second block the CM SAF FCDR and the last block the CSU FCDR.

	F16	F17	F18
Bias [K]	0. 16	0. 54	- 0. 70
RSD [K]	0. 77	0. 61	0. 71
MAD [K]	0. 53	0. 63	0. 77
max absolute inter-sensor Bias [K]	- 0. 86	1. 24	1. 24
Bias [K]	0. 00	- 0. 05	0. 07
RSD [K]	0. 56	0. 57	0. 61
MAD [K]	0. 38	0. 39	0. 42
max absolute inter-sensor Bias [K]	0. 07	0. 12	0. 12
Trend [K/dec]	- 0. 02 ($\alpha > 30\%$)	- 0. 04 ($\alpha > 30\%$)	- 0. 07 ($\alpha > 30\%$)
Bias [K]	- 0. 08	- 0. 12	0. 21
RSD [K]	0. 62	0. 52	0. 69
MAD [K]	0. 43	0. 38	0. 50
max absolute inter-sensor Bias [K]	0. 29	0. 33	0. 33

Table 6: Statistics of instrument differences for SSMIS channel 19h GHz. The numbers represent percentiles of absolute differences less than 1K, 2K, and 3K of all monthly mean grid boxes between two instruments.

	F16	F17	F18
F13	59. 9 83. 9 92. 9	51. 5 74. 7 85. 9	
F14	56. 7 81. 6 91. 7	46. 9 70. 9 83. 1	
F16		67. 5 87. 3 94. 3	66. 6 88. 0 95. 3
F17			63. 8 87. 3 95. 0

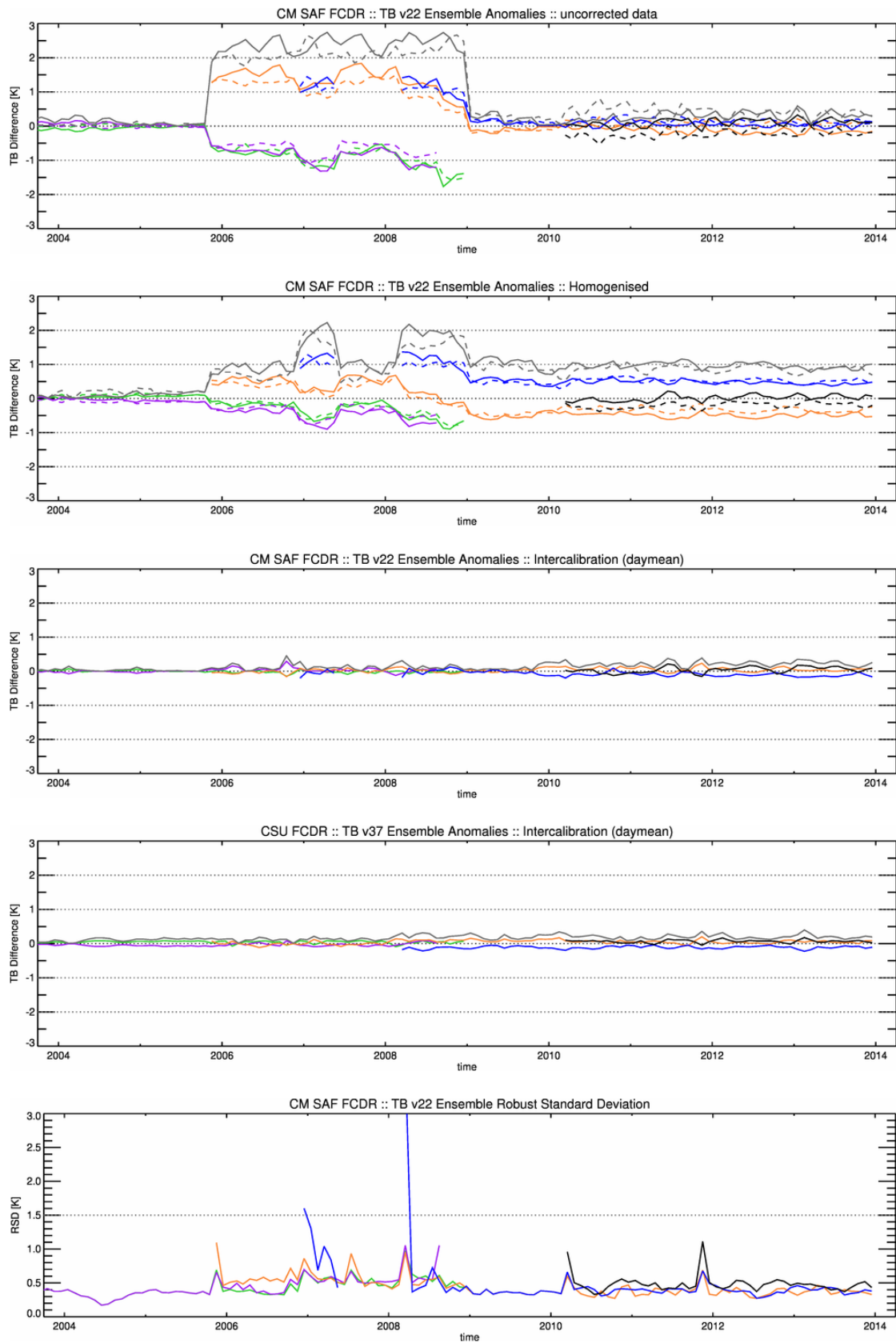


Figure 8: Same as Figure 6, but for SSM/I & SSMIS channel 22v GHz.

Table 7: Statistics of the ensemble anomalies for SSMIS channel 22v GHz. The first block shows the original RDR with EIA normalized, the second block the CM SAF FCDR and the last block the CSU FCDR.

	F16	F17	F18
Bias [K]	- 0. 23	0. 57	- 0. 09
RSD [K]	0. 60	0. 47	0. 51
MAD [K]	0. 48	0. 61	0. 35
max absolute inter-sensor Bias [K]	0. 80	0. 80	0. 66
Bias [K]	0. 04	- 0. 07	0. 05
RSD [K]	0. 42	0. 40	0. 46
MAD [K]	0. 29	0. 28	0. 32
max absolute inter-sensor Bias [K]	0. 11	0. 12	0. 12
Trend [K/dec]	0. 09 ($\alpha > 30\%$)	- 0. 24 ($\alpha < 5\%$)	- 0. 34 ($\alpha < 5\%$)
Bias [K]	0. 08	- 0. 11	0. 06
RSD [K]	0. 41	0. 39	0. 40
MAD [K]	0. 28	0. 28	0. 28
max absolute inter-sensor Bias [K]	0. 19	0. 19	0. 17

Table 8: Statistics of instrument differences for SSMIS channel 22v GHz. The numbers represent percentiles of absolute differences less than 1K, 2K, and 3K of all monthly mean grid boxes between two instruments.

	F16	F17	F18
F13	71. 4 91. 5 97. 1	61. 7 83. 1 91. 2	
F14	68. 7 90. 4 96. 6	57. 0 79. 6 89. 0	
F16		78. 3 93. 4 97. 4	77. 7 94. 6 98. 3
F17			76. 9 94. 4 98. 3

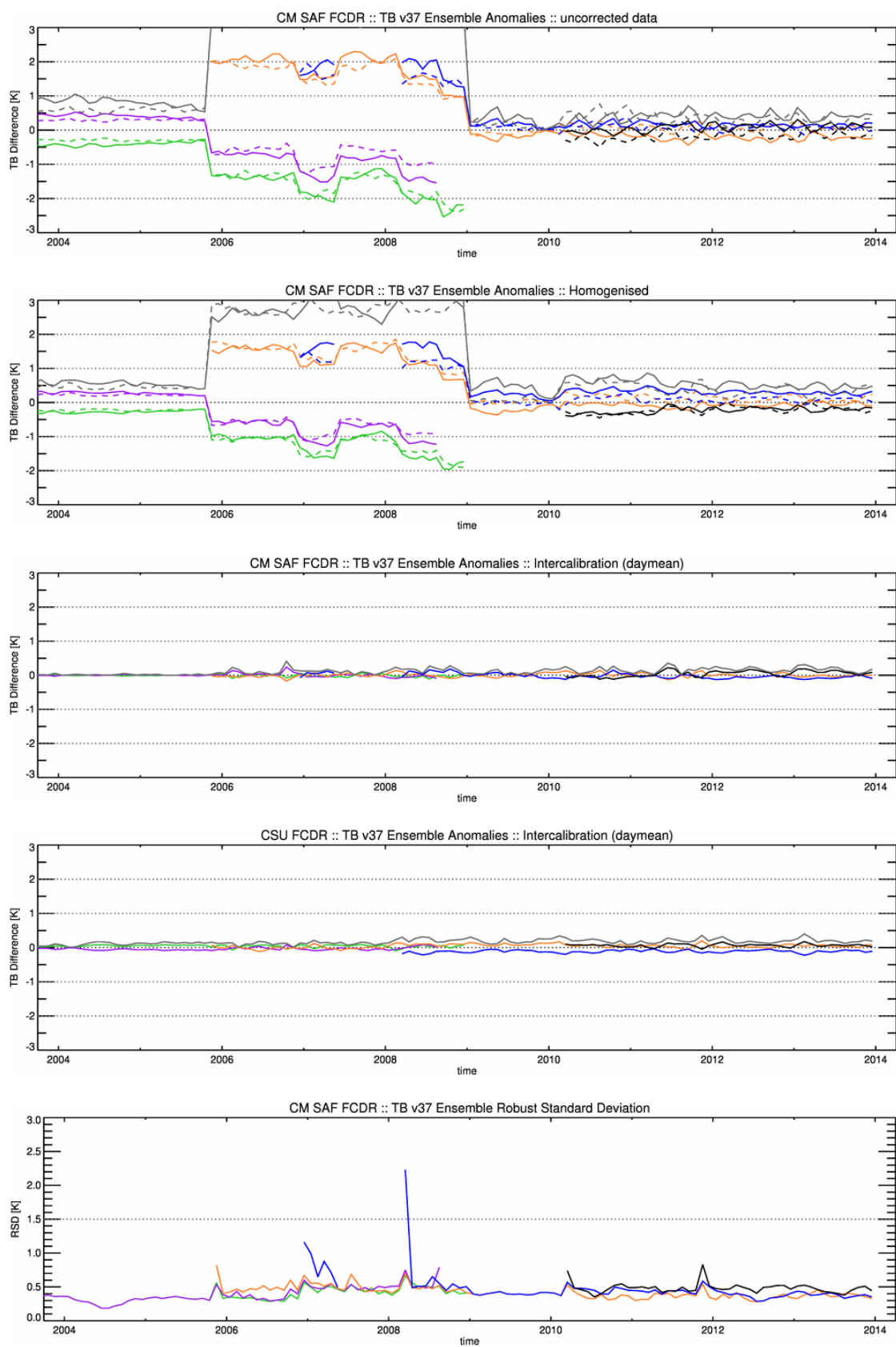


Figure 9: Same as Figure 6, but for SSM/I & SSMIS channel 37v GHz.

Table 9: Statistics of the ensemble anomalies for SSMIS channel 37v GHz. The first block shows the original RDR with EIA normalized, the second block the CM SAF FCDR and the last block the CSU FCDR.

	F16	F17	F18
Bias [K]	0. 31	0. 30	- 0. 22
RSD [K]	0. 82	0. 58	0. 49
MAD [K]	0. 50	0. 43	0. 37
max absolute inter-sensor Bias [K]	0. 53	0. 52	0. 53
Bias [K]	0. 00	- 0. 02	0. 05
RSD [K]	0. 41	0. 44	0. 47
MAD [K]	0. 28	0. 30	0. 32
max absolute inter-sensor Bias [K]	0. 05	0. 07	0. 05
Trend [K/dec]	0. 02 ($\alpha > 30\%$)	- 0. 23 ($\alpha < 5\%$)	0. 39 ($\alpha < 0. 03\%$)
Bias [K]	0. 05	- 0. 11	0. 07
RSD [K]	0. 36	0. 36	0. 40
MAD [K]	0. 25	0. 26	0. 28
max absolute inter-sensor Bias [K]	0. 16	0. 18	0. 18

Table 10: Statistics of instrument differences for SSMIS channel 37v GHz. The numbers represent percentiles of absolute differences less than 1K, 2K, and 3K of all monthly mean grid boxes between two instruments.

	F16	F17	F18
F13	77. 4 94. 9 98. 7	66. 0 88. 5 95. 2	
F14	73. 8 93. 6 98. 2	63. 2 86. 5 93. 9	
F16		79. 0 95. 2 98. 5	79. 1 96. 3 99. 1
F17			75. 9 95. 2 98. 8

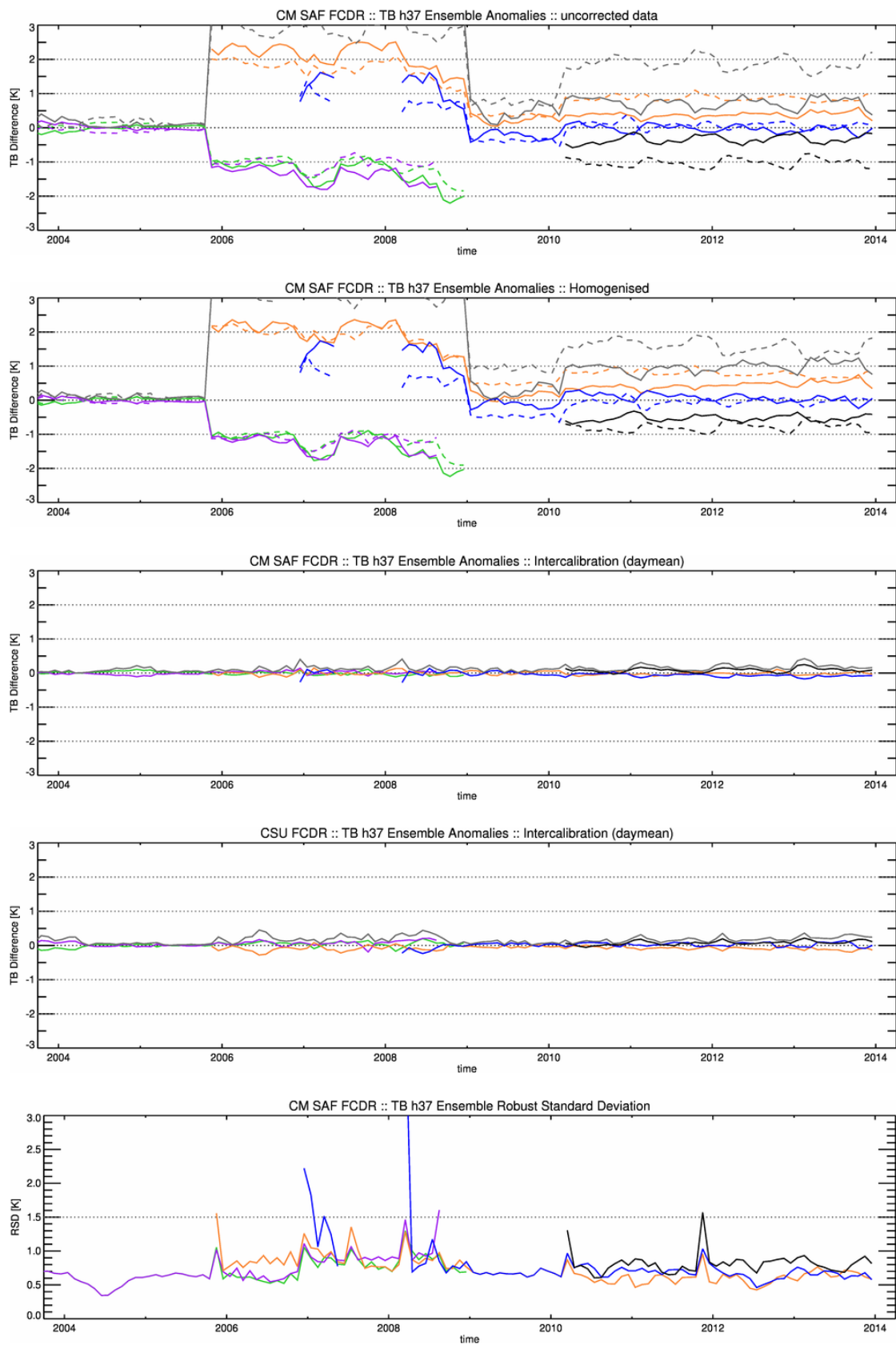


Figure 10: Same as Figure 6, but for SSM/I & SSMIS channel 37h GHz.

Table 11: Statistics of the ensemble anomalies for SSMIS channel 37h GHz. The first block shows the original RDR with EIA normalized, the second block the CM SAF FCDR and the last block the CSU FCDR.

	F16	F17	F18
Bias [K]	0. 93	0. 09	- 0. 68
RSD [K]	1. 08	0. 87	0. 90
MAD [K]	1. 01	0. 59	0. 81
max absolute inter-sensor Bias [K]	1. 61	0. 77	1. 61
Bias [K]	- 0. 01	- 0. 05	0. 09
RSD [K]	0. 70	0. 73	0. 79
MAD [K]	0. 48	0. 50	0. 54
max absolute inter-sensor Bias [K]	0. 10	0. 14	0. 14
Trend [K/dec]	- 0. 02 ($\alpha > 30\%$)	- 0. 18 ($\alpha < 5\%$)	0. 03 ($\alpha > 30\%$)
Bias [K]	- 0. 07	0. 01	0. 08
RSD [K]	0. 74	0. 75	0. 77
MAD [K]	0. 51	0. 51	0. 52
max absolute inter-sensor Bias [K]	0. 15	0. 07	0. 15

Table 12: Statistics of instrument differences for SSMIS channel 37h GHz. The numbers represent percentiles of absolute differences less than 1K, 2K, and 3K of all monthly mean grid boxes between two instruments.

	F16	F17	F18
F13	53. 6 79. 1 90. 2	45. 6 70. 7 83. 4	
F14	49. 9 75. 8 88. 2	42. 2 67. 4 80. 7	
F16		59. 3 82. 8 92. 0	56. 8 82. 7 92. 7
F17			53. 4 81. 0 92. 1

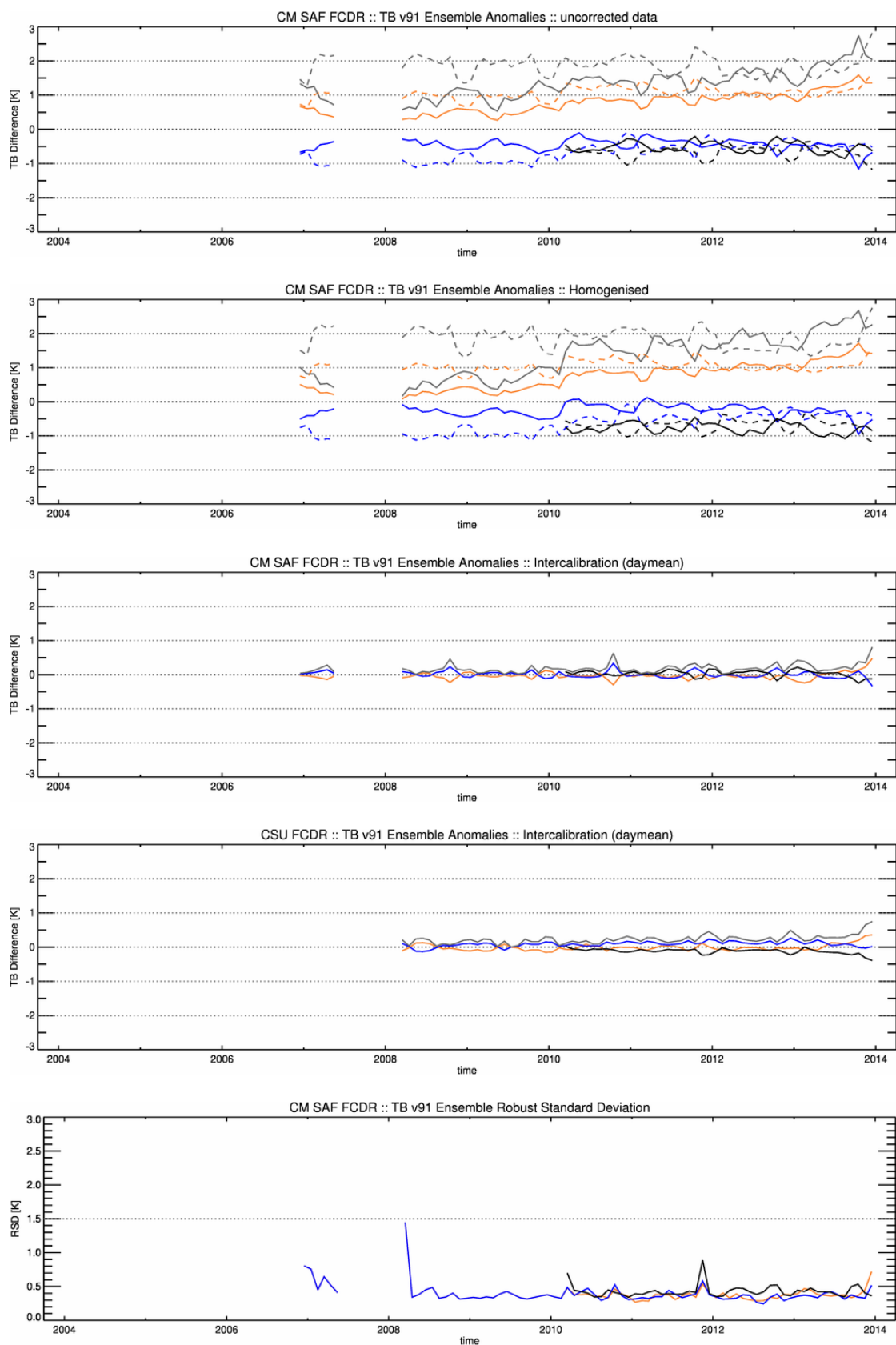


Figure 11: Same as Figure 6, but for SSMIS channel 91v GHz.

Table 13: Statistics of the ensemble anomalies for SSMIS channel 91v GHz. The first block shows the original RDR with EIA normalized, the second block the CM SAF FCDR and the last block the CSU FCDR.

	F16	F17	F18
Bias [K]	0. 92	- 0. 44	- 0. 73
RSD [K]	0. 47	0. 44	0. 46
MAD [K]	0. 93	0. 47	0. 74
max absolute inter-sensor Bias [K]	1. 65	1. 36	1. 65
Bias [K]	- 0. 04	0. 01	0. 04
RSD [K]	0. 38	0. 38	0. 42
MAD [K]	0. 26	0. 26	0. 29
max absolute inter-sensor Bias [K]	0. 08	0. 05	0. 08
Trend [K/dec]	0. 06 ($\alpha > 30\%$)	- 0. 14 ($\alpha < 5\%$)	0. 04 ($\alpha > 30\%$)
Bias [K]	- 0. 01	0. 09	- 0. 12
RSD [K]	0. 33	0. 37	0. 40
MAD [K]	0. 23	0. 26	0. 29
max absolute inter-sensor Bias [K]	0. 11	0. 21	0. 11

Table 14: Statistics of instrument differences for SSMIS channel 91v GHz. The numbers represent percentiles of absolute differences less than 1K, 2K, and 3K of all monthly mean grid boxes between two instruments.

	F16	F17	F18
F16		83. 3 96. 9 99. 0	82. 0 97. 5 99. 4
F17			82. 2 97. 4 99. 4

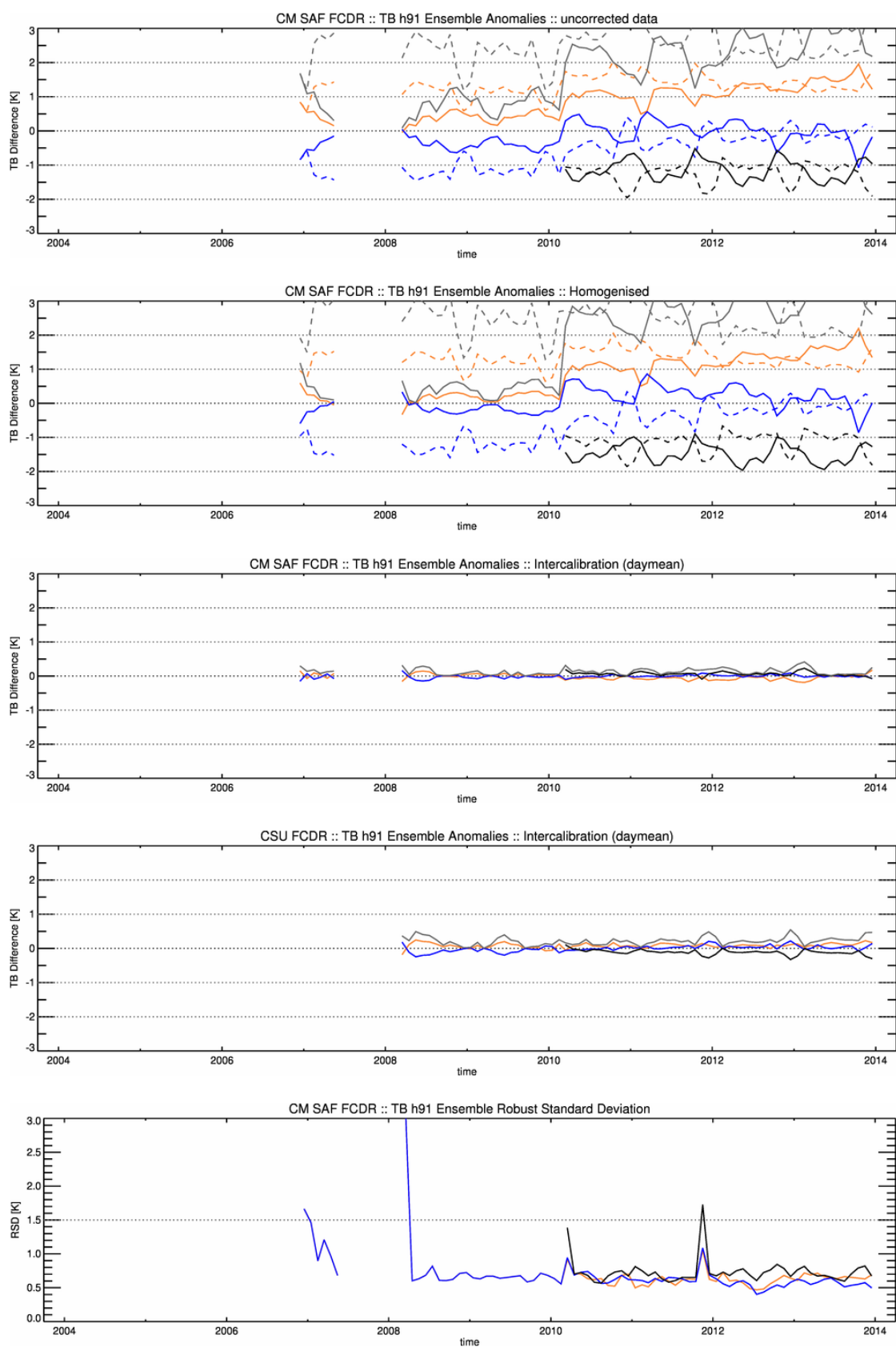


Figure 12: Same as Figure 6, but for SSMIS channel 91h GHz.





 	EUMETSAT SAF on CLIMATE MONITORING Validation Report Microwave Radiance FCDR R2	Doc.No.: SAF/CM/DWD/VAL/FCDR_SSMIS Issue: 1.1 Date: 2015-02-26
---	--	--

Table 15: Statistics of the ensemble anomalies for SSMIS channel 91h GHz. The first block shows the original RDR with EIA normalized, the second block the CM SAF FCDR and the last block the CSU FCDR.

	F16	F17	F18
Bias [K]	1. 14	- 0. 27	- 1. 31
RSD [K]	0. 80	0. 95	0. 92
MAD [K]	1. 17	0. 67	1. 33
max absolute inter-sensor Bias [K]	2. 45	1. 41	2. 45
Bias [K]	- 0. 03	- 0. 01	0. 06
RSD [K]	0. 66	0. 65	0. 71
MAD [K]	0. 45	0. 44	0. 48
max absolute inter-sensor Bias [K]	0. 09	0. 07	0. 09
Trend [K/dec]	- 0. 21 ($\alpha > 5\%$)	0. 08 ($\alpha < 5\%$)	- 0. 18 ($\alpha > 5\%$)
Bias [K]	0. 08	0. 00	- 0. 11
RSD [K]	0. 59	0. 62	0. 72
MAD [K]	0. 41	0. 41	0. 50
max absolute inter-sensor Bias [K]	0. 19	0. 11	0. 19

Table 16: Statistics of instrument differences for SSMIS channel 91h GHz. The numbers represent percentiles of absolute differences less than 1K, 2K, and 3K of all monthly mean grid boxes between two instruments.

	F16	F17	F18
F16		61. 3 85. 7 94. 1	58. 9 85. 8 94. 9
F17			59. 7 85. 8 94. 9

 	EUMETSAT SAF on CLIMATE MONITORING Validation Report Microwave Radiance FCDR R2	Doc.No.: SAF/CM/DWD/VAL/FCDR_SSMIS Issue: 1.1 Date: 2015-02-26
---	--	--

III-3 Conclusions

The CM SAF FCDR of SSMIS brightness temperatures has been evaluated to analyse the homogeneity, consistency and the stability of the developed inter-calibration model. The CM SAF FCDR has been compared to the original RDR and another available FCDR from CSU. The main distinction between both FCDRs is found in the applied inter-calibration method. The inter-calibration method developed for the CM SAF FCDR explicitly includes all possible surface types to account for the entire natural distribution of brightness temperatures from radiometric cold scenes (rain-free ocean) to radiometric warm scenes (vegetated land surfaces). In contrast to this, the inter-calibration method developed at CSU is limited to the rain-free brightness temperatures range observed by the TMI instrument because this is used as transfer standard. This practically limits the CSU inter-calibration to the radiometric cold end of the natural spectrum and hampers a correct consideration of possible scene dependencies.



In section III-2.2 it is shown that the CM SAF inter-calibration model is applicable over all surface types. While both evaluated FCDRs show similar characteristics over oceans (radiometric cold scenes), land and sea ice covered areas (radiometric warm scenes) remain strongly biased in the CSU FCDR. As discussed in section III-2.2, polarization double difference maps are used as a cross check how the inter-calibration performs for the different surface types. This comparison proves that the CM SAF inter-calibration model leads to a clear improvement over the CSU FCDR, particular for land and sea ice covered regions, as it better accounts for the strong scene dependent bias of the SSMIS compared to the CSU method. While the CM SAF method removes most of observed differences over warm scenes, resulting in consistent characteristics in vertically and horizontally polarized channels, the CSU FCDR depicts offsets in the order of up to 2 K after inter-calibration.

The consistency and homogeneity of both FCDRs and the uncorrected RDR were statistically analysed to demonstrate the improvement of the re-processed data records and compliance with the user requirements. Those requirements are defined in terms of mean absolute systematic inter-satellite deviations and decadal stability.

The observed differences in the RDR range between 0.5 K to 2.5 K, depending on channel and instrument, but generally the differences are smaller within the SSMIS series as compared to the inter-sensor difference to the SSM/I family. The overall mean differences in the CM SAF FCDR between the different sensors have been reduced to below 0.1 K, which is a significant improvement over the RDR. The mean RSD for all channels and instruments has been significantly reduced. The observed remaining variability in the inter-calibrated TBs is mainly caused by the natural variability due to overpass time differences and sampling differences. Except for two channels of the F18, no significant trend above 0.03 K/decade can be observed, keeping in mind that the time period of F18 is too short for a reliable decadal trend estimate.

Finally it can be concluded that this FCDR is providing a greatly improved quality of the SSMIS brightness temperatures as compared to original raw data records and fulfils the aimed requirements. It seamlessly extends the current SSM/I FCDR until end of 2013.

Additionally to the inter-sensor comparisons, a more complete analysis of each individual channel across the sensors for the complete time period will be performed for the next release of the microwave radiance FCDR. This allows a better characterisation of the long-term FCDR stability. The next release will extend the SSMIS covered time period by two years and also include the Scanning Multichannel Microwave Radiometer (SMMR). The combined FCDR will then cover the time period from October 1978 to December 2015. The validation will then be extended to compare the observed brightness temperatures against simulated brightness temperatures using ERA20C.

 	EUMETSAT SAF on CLIMATE MONITORING Validation Report Microwave Radiance FCDR R2	Doc.No.: SAF/CM/DWD/VAL/FCDR_SSMIS Issue: 1.1 Date: 2015-02-26
---	--	--

III-4 References

- Andersson, A., Fennig, K., Klepp, C., Bakan, S., Graßl, H., and Schulz, J.: The Hamburg Ocean Atmosphere Parameters and Fluxes from Satellite Data – HOAPS-3, *Earth Syst. Sci. Data*, 2, 215-234, doi:10.5194/essd-2-215-2010, 2010.
- Andersson, A., C. Klepp, K. Fennig, S. Bakan, H. Graßl, and J. Schulz: Evaluation of HOAPS-3 ocean surface freshwater flux components, *Journal of Applied Meteorology and Climatology*, 50, 379-398, doi:10.1175/2010JAMC2341.1, 2011.
- Berg, W., Sapiano, M. R. P. ; Horsman, J. ; Kummerow, C., 2012: Improved Geolocation and Earth Incidence Angle Information for a Fundamental Climate Data Record of the SSM/I Sensors, *IEEE Transactions on Geoscience and Remote Sensing*, Early online release, doi: 10.1109/TGRS.2012.2199761.
- Berg, W., 2013: Fundamental Climate Data Record (FCDR) for the Special Sensor Microwave Imager/Sounder (SSMIS), *Climate Algorithm Theoretical Basis Document (C-ATBD)*, CDR Program Document Number: CDRP-ATBD-0338
- Furhop, R. and Simmer, C.: SSM/I Brightness Temperature Corrections for Incidence Angle Variations, *J. Atmos. Oceanic Technol.*, 13, 246–254, 1996.
- Hollinger, J., Poe, G..A.: *Special Sensor Microwave/Imager User's Guide*, Naval Research Laboratory Report, Washington DC, 1987.
- Semunegus, H: Remote Sensing Systems Version-6 Special Sensor Microwave/Imager Fundamental Climate Data Record, *Climate Algorithm Theoretical Basis Document, Climate Data Record (CDR) Program*, CDRP-ATBD-0100, 2011.

III-5 Glossary

APC	Antenna Pattern Correction
ATBD	Algorithm Theoretical Baseline Document
CM SAF	Satellite Application Facility on Climate Monitoring
CDOP	Continuous Development and Operations Phase
CSU	Colorado State University
DMSP	Defense Meteorological Satellite Program
DWD	Deutscher Wetterdienst (German MetService)
ECI	Earth-centred inertial
ECMWF	European Centre for Medium Range Forecast
ECV	Essential Climate Variable
EIA	Earth Incidence Angle
EPS	European Polar System
EUMETSAT	European Organisation for the Exploitation of Meteorological Satellites
FCDR	Fundamental Climate Data Record
FMI	Finnish Meteorological Institute
FOV	Field of view
GCOS	Global Climate Observing System
GLOBE	The Global Land One-kilometer Base Elevation
HOAPS	The Hamburg Ocean Atmosphere Fluxes and Parameters from Satellite data
IOP	Initial Operations Phase
KNMI	Koninklijk Nederlands Meteorologisch Instituut
MAD	Median absolute deviation
MD5	Message-Digest Algorithm 5
MSG	Meteosat Second Generation
NASA	National Aeronautics and Space Administration
NCEP	National Centers for Environmental Prediction
NDBC	National Data Buoy Center
NESDIS	National Environmental Satellite, Data, and Information System
NMHS	National Meteorological and Hydrological Services
NOAA	National Oceanic & Atmospheric Administration
NWP	Numerical Weather Prediction
PRD	Product Requirement Document
PUM	Product User Manual

QC	Quality Control
RDR	Raw Data Record
RMIB	Royal Meteorological Institute of Belgium
RMS	Root Mean Square
RSD	Robust Standard Deviation
RSS	Remote Sensing Systems
SAF	Satellite Application Facility
SI	Système international d'unités
SMHI	Swedish Meteorological and Hydrological Institute
SMMR	Scanning Multichannel Microwave Radiometer
SSM/I	Special Sensor Microwave Imager
SSMIS	Special Sensor Microwave Imager Sounder
TA	Antenna Temperature
TB	Brightness Temperature
TDR	Temperature Data Records